Scientific paper

Synthetic Optimization and Antibacterial Activity of Novel Benzodioxepine-Biphenyl Amide Derivatives

Shao-Peng Yan,^{1,2,3} Zhi-Yu Zhu,^{1,2,3} Qi-Ke Jia,^{2,3} Rui-Ying Ji,^{1,2,3} Ya-Pin Wang,^{1,2,3} Dan He,^{1,2,3} Rong Wang^{1,2,3*} Xiao-Jun Xu⁴ and Yang Zhou^{1,2,3,5*}

¹ Cixi Biomedical Research Institute, Wenzhou Medical University, Ningbo, 315300, China

² Laboratory of Advanced Theranostic Materials and Technology, Ningbo Institute of Materials Technology and Engineering, Chinese Academy of Sciences, Ningbo, 315300, China

³ Ningbo Cixi Institute of Biomedical Engineering, Ningbo, 315300, China

⁴ College of Pharmaceutical Engineering and Biotechnology, Zhejiang Pharmaceutical University, Ningbo, 315500, China

⁵ Pingshan Translational Medicine Center, Shenzhen Bay Laboratory, Shenzhen, 518118 China

* Corresponding author: E-mail: rong.wang@nimte.ac.cn (R. Wang), zhouyang876@nimte.ac.cn (Y. Zhou)

Received: 04-26-2024

Abstract

The biosynthesis of fatty acids is an important metabolic pathway in bacterial organisms. Previous studies have highlighted the synthesis of antimicrobial compounds anchored in the benzodioxepin scaffold and known for their pronounced antibacterial properties. Based on this fundamental knowledge, a series of eight innovative benzodioxepin-biphenyl amide derivatives were carefully designed and synthesized in the current research work. This was achieved through a sophisticated optimization of the synthetic methods. The scope of this study extends to a rigorous evaluation of the antibacterial properties and biocompatibility of the above-mentioned new derivatives. In particular, compound E4 proved to be an extremely effective antimicrobial agent. In addition to a detailed elucidation of the crystalline architecture of compound E4, a thorough docking study was also carried out to investigate the interactions with the enzyme FabH.

Keywords: Benzodioxepine amide, biphenyl, Suzuki coupling, antibacterial activity, FabH inhibitor

1. Introduction

Fatty acid biosynthesis is an essential metabolic pathway that is crucial for the survival and growth of various organisms and exhibits remarkable biodiversity. 1-3 This pathway is mainly facilitated by two enzyme systems: fatty acid synthase I (FAS I) and fatty acid synthase II (FAS II). FAS I, which is found primarily in mammals and yeasts, uses a multifunctional protein complex in which each step of synthesis is catalyzed by different domains within a single polypeptide. In contrast, FAS II, found in bacteria and plants, utilizes a series of independent, monofunctional enzymes, each responsible for specific steps of the process. 4-6 Targeting these monofunctional enzymes in bacterial FAS II has proven to be a viable strategy for the development of new antimicrobial agents with lower toxicity to humans, highlighting the therapeutic potential of this approach. Among these enzymes, β-ketoacyl-ACP

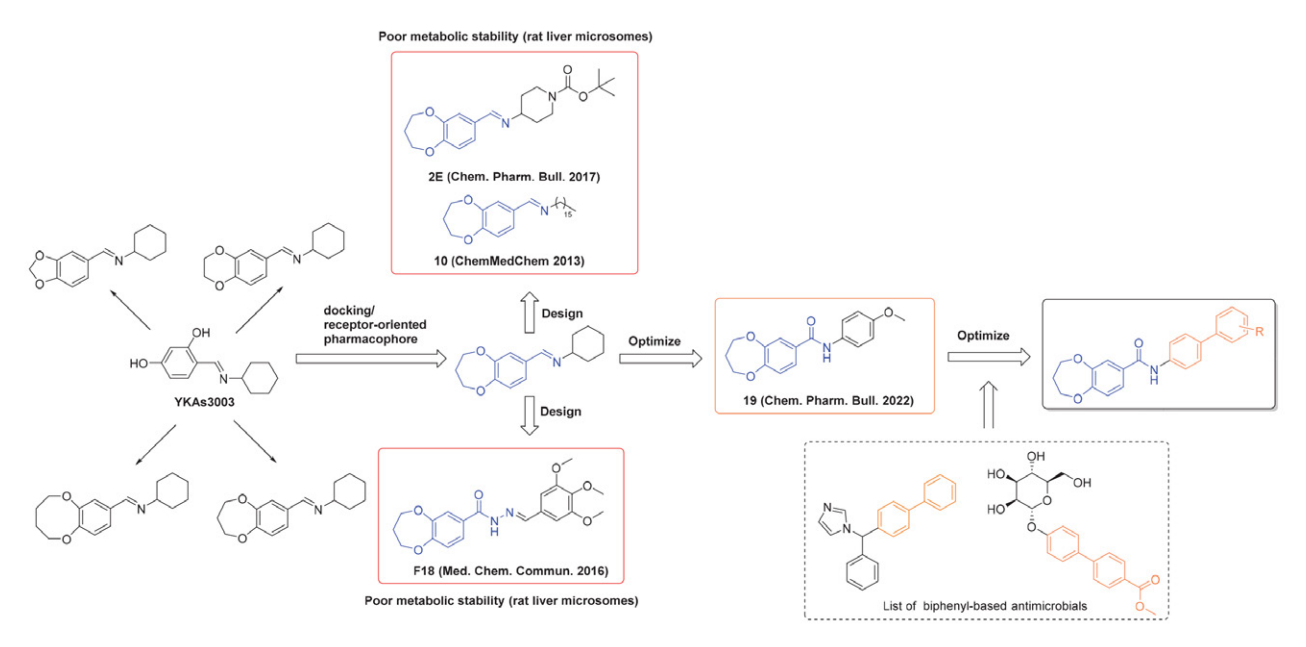
synthase III (FabH) is increasingly recognized for its critical role in initiating fatty acid synthesis in bacteria, making it a priority target for antimicrobial drug development. As an essential β-ketoacyl-ACP synthase, FabH catalyzes the initiation of fatty acid synthesis through the use of acyl-CoA, setting the pace for subsequent elongation cycles. In contrast to its homologues FabF and FabB, which elongate the fatty acid chain using acyl-ACP, FabH exclusively utilizes acetyl-CoA, highlighting its unique substrate preference.^{7,8} Furthermore, FabH is ubiquitously present in a variety of clinically important pathogens, including Gram-positive and Gram-negative bacteria, chlamydiae, anaerobes, mycobacteria, and protozoa. In addition, the gene sequences and three-dimensional structures of FabH are conserved in these pathogens, whereas homologous proteins are absent in humans. Remarkably, the active site residues of FabH are consistent in both Gram-positive and Gram-negative bacteria. 9-12 All these features underscore its potential as a therapeutic target.

In preliminary studies, we have used the structural basis of YKAs3003 to develop a series of novel Schiff base derivatives. Using the CDOCKER computational platform, we found that derivatives with a benzodioxepin scaffold exhibited significant alignment (1.57282) and reduced binding energies (-28.4496 kcal/mol) compared to the pharmacophore model of the FabH enzyme, suggesting their potential as potent FabH inhibitors. 13-15 We then investigated the antimicrobial activity of these Schiff bases and their hydrazone analogs. These compounds exhibited considerable activity against various Gram-positive and Gram-negative bacteria. Despite the recognized role of Schiff and hydrazone moieties as essential pharmacophores in numerous antimicrobial agents, including those targeting FabH, their susceptibility to hepatic metabolic degradation has limited further in vivo studies. To address the observed metabolic instability of Schiff and hydrazone groups in antimicrobial agents, our research has focused on the incorporation of more stable amide linkages. This modification has resulted in lead compounds with enhanced in vitro antibacterial activity, which is a promising direction for further antimicrobial exploration.¹⁶ The biphenyl motif, characterized by two benzene rings linked by a single bond, is a structural feature commonly observed in various antimicrobial compounds. 17-19 Its inherent chemical stability and ability to form multiple interactions with bacterial targets are critical properties that influence our drug design. Compounds with the biphenyl structure are known to exert antimicrobial effects via multiple mechanisms, including disruption of cell walls or membranes and inhibition of protein and nucleic acid synthesis.^{20–25} Building on these findings, our current strategy

utilizes a combinatorial pharmacophore model in which the amide-modified benzodioxepin core is combined with the biphenyl scaffold. The details of this design approach are shown in Scheme 1. Using an optimized synthetic route, this study starts with the reaction of benzodioxepine with p-bromoaniline to synthesize the corresponding amide derivatives. This step is followed by a Suzuki-Miyaura coupling reaction with phenylboronic acid, which aims to determine the most favorable synthesis conditions. 26,27 This methodological approach not only expands the substrate range but also improves the comprehensive exploration of the antimicrobial efficacy and target specificity of the derivatives. The results obtained provide a solid basis for the development of new benzodioxepin-biphenyl lead compounds specifically targeting the FabH enzyme.

2. Results and Discussion

In previous studies, the synthesis of benzodioxepine-biphenylamide derivatives was first carried out using a Suzuki coupling to produce an aminated biphenyl. This intermediate was then condensed with the carboxylic acid of benzodioxepine to obtain the desired amide derivatives. In this study, a critical re-evaluation of the synthetic sequence revealed an alternative approach in which the reaction begins with the coupling of the benzodioxepine carboxylic acid and p-bromoaniline to form the amide. This amide is then used in a Suzuki coupling with various phenylboronic acid derivatives. This revised methodology not only facilitated the purification of the final product, but also significantly reduced the occurrence of side reactions, increasing the overall purity of the benzodioxepine



Scheme 1. The design strategy of benzodioxepin-biphenyl compounds as FabH inhibitors.

Table 1. Optimization of the reaction conditions.^a

Entry	[Pd]	Amt of cat. (mol%)	Base	Solvent	T (°C)	Yield (%)b
1	Pd(PPh ₃) ₄	5	K ₂ CO ₃	1,4-dioxane	80	21
2	$Pd(OAc)_2$	5	K_2CO_3	1,4-dioxane	80	17
3	Pd(dba) ₂	5	K_2CO_3	1,4-dioxane	80	45
4	Pd(dppf)Cl ₂ ·DCM	1 5	K_2CO_3	1,4-dioxane	80	65
5	Pd/C	5	K_2CO_3	1,4-dioxane	80	<5
6	Pd(dppf)Cl ₂ ·DCM	1 5	Na ₂ CO ₃	1,4-dioxane	80	81
7	Pd(dppf)Cl ₂ :DCM	1 5	Cs ₂ CO ₃	1,4-dioxane	80	93
8	Pd(dppf)Cl ₂ ·DCM	1 5	AcOK	1,4-dioxane	80	72
9	Pd(dppf)Cl ₂ ·DCM	1 5	Et_3N	1,4-dioxane	80	54
10c	Pd(dppf)Cl ₂ ·DCM	1 5	Cs_2CO_3	THF	65	69
11	Pd(dppf)Cl ₂ ·DCM	1 5	Cs_2CO_3	EtOH	70	37
11	Pd(dppf)Cl ₂ ·DCM		Cs_2CO_3	Toluene	90	37
12	Pd(dppf)Cl ₂ ·DCM		Cs_2CO_3	1,4-dioxane	80	79
13	Pd(dppf)Cl ₂ DCM		Cs_2CO_3	1,4-dioxane	80	94

^a All reactions were carried out at a scale of 0.5 mmol of compound D. ^bGC yield.

biphenylamide derivatives. By strategically positioning the Suzuki coupling as the final step of the synthesis, process optimization led to a more efficient route to produce the desired compounds. Thus, we began our synthesis efforts with the preparation of N-(4-bromophenyl)-3,4-dihydro-2H-benzo[b][1,4]dioxepin-7-carboxamide (compound \mathbf{D}). The synthetic pathway is shown in Figure 1, where we used compound \mathbf{D} together with phenylboronic acid as substrates to optimize the conditions for Suzuki coupling.

In our study, shown in Table 1, we have investigated in detail the influence of various parameters on the Suzuki coupling reactions. Using a solvent system of 1,4-dioxane and water at a ratio of 20:1 and heating the mixture for five hours at a constant palladium catalyst concentration of 5 mol%, we first focused on evaluating the effects of different palladium catalysts on the reaction efficiency. As described in entries 1 through 5, a series of palladium catalysts were tested for their ability to facilitate the synthesis of benzodioxepine biphenyl compounds, herein referred to as compound E. In particular, Pd(dppf)Cl₂·DCM proved to be the most effective with a gas chromatographic yield of 65 %. The effects of different bases on the yield were then investigated, as documented in entries 4 and 6 to 9. When investigating the influence of base selection on the Suzuki coupling reactions, we found a positive correlation between the alkalinity of the inorganic bases and the resulting product yield. In particular, the replacement of potassium carbonate (K₂CO₃) with sodium carbonate (Na₂CO₃)

or cesium carbonate (Cs₂CO₃) led to a progressive improvement in yield, with Cs₂CO₃ producing the most significant increase. In contrast, the use of organic bases such as potassium acetate (AcOK) and triethylamine (Et₃N) was found to negatively affect the yield. Further investigations focused on the role of the solvent for the catalytic efficiency. Changing the solvent from 1,4-dioxane to toluene, THF or ethanol did not improve the yield. In addition, our analysis of the optimal catalyst concentration revealed that decreasing the Pd(dppf)Cl₂·DCM concentration from 5 mol% to 4 mol% significantly decreased the yield, while increasing the concentration to 6 mol% did not significantly increase the yield. Therefore, we determined that the optimal catalyst concentration was 5 mol%. After careful optimization of the Suzuki coupling reaction parameters, we established an effective protocol involving a catalyst concentration of 5 mol% Pd(dppf)Cl₂·DCM, the use of two equivalents of Cs₂CO₃, and a solvent system of 1,4-epoxycyclohexane and water in a volume ratio of 20:1. This mixture was refluxed at 80 °C for five hours. Under these optimized conditions, a comprehensive evaluation of the substrate scope was performed. The results presented in Table 2 show that substrates with a variety of substituent groups (E1-8) consistently gave products with isolated yields between 79% and 95%.

The investigation of the antimicrobial efficacy and biocompatibility of eight novel benzodioxepine-carbamide diphenyl derivatives is described, with the relevant results listed in Table 3. The octanol-water partition coeffi-

Table 2. Pd complex-catalyzed benzylic oxidation.^a

cient (AlogP) serves as an essential index for measuring the lipophilicity of active pharmaceutical ingredients and has a profound impact on their absorption, distribution, metabolism and excretion (ADME) properties. Optimal lipophilicity is crucial for facilitating the passage of drugs through cell membranes and thus improving their bioavailability. In this series, all compounds exhibited AlogP values below 7, which ensures a favorable lipid-water balance that supports adequate membrane permeability while mitigating the risks associated with excessive lipophilicity, such as insolubility and bioaccumulation. In addition, these derivatives exhibited minimal cytotoxicity to NIH-3T3 mouse fibroblast cells, with IC50 values above 100 uM, opening promising prospects for subsequent in vivo efficacy studies. However, the study showed that the antimicrobial efficacy of the investigated compounds is significantly influenced by the nature of the substituents attached to the biphenyl group. This observation emphasizes the central role of chemical substituents in modulating biological activities and illustrates a complex relationship between molecular architecture and antimicrobial strength. In particular, the parent compound E1 and its

chlorine-substituted derivative E2 showed lower antimicrobial activity. This lower potency can be primarily attributed to the insufficient electronic effects required for optimal interaction with biological targets. In addition, the ability of chlorine to withdraw electrons was found to be relatively weak, resulting in less effective non-covalent interactions with the active sites of these targets. Our study also showed marked differences in the antimicrobial efficacy of biphenyl derivatives when modified with nitro (E3) and cyano (E4) substituents. The nitro group $(-NO_2)$, known for its strong electron-withdrawing properties, is involved in conjugation processes that reduce the electron density around the biphenyl core. This reduction in electron density likely facilitates more effective interactions with biological targets and increases antimicrobial activity. In contrast, the cyano group (-CN) serves as a milder electron attractor. Its less pronounced effect preserves the electron density of the biphenyl backbone to a greater extent, potentially maintaining more balanced interactions with biological targets without compromising molecular stability too much. In addition, a comparative analysis of compounds containing trifluoromethoxy (-OCF₃) and trifluo-

Comp.	Alog P	Minimum inhibitory concentrations (μg/mL) Gram-negative Gram-positive			0	Cytotoxicity IC ₅₀ (μM)	
		E. coli	P. aeruginosa	S. aureus	S. pneumoni	ae	
E1	4.12	>100	>100	50	50	117.3±7.5	
E2	4.68	50	>100	50	>100	158.9±11.8	
E3	4.11	50	25	12.5	50	176.8±6.9	
E4	4.16	6.25	12.5	12.5	25	124.6±8.4	
E5	5.65	>100	25	50	50	161.4±5.2	

12.5

25

50

50

25

>100

Table 3. Antibacterial activity and cytotoxicity of synthetic compounds.

12.5

12.5

50

romethyl (-CF₃) groups showed considerable differences in their antimicrobial efficacy despite their structural similarities. In particular, the compounds with the OCF₃ group (E5) showed significantly lower activity than their CF₃-substituted counterparts (E6). This observation suggests that even subtle differences in the electronic properties of the substituent groups can have significant effects on the biological properties of the molecules, emphasizing the importance of precise molecular design for the development of effective antimicrobial agents.

5.04

5.60

5.24

E6

E7

E8

The crystal structures of compound **E4** were determined by X-ray diffraction analysis to better predict and

analyze the binding of **E4** to the target in the future study. The crystal data shown in Table 4 and Figure 2 represent the perspective views of **E4** with the atomic labeling system. The crystallographic data has been deposited at the Cambridge Crystallographic Data Center (CCDC, number 2348536).

124.3±9.8

139.5±8.1

146.9±7.8

25

12.5

>100

To elucidate the binding pattern between the target protein and the small molecules, molecular docking was performed using the crystal structure of *E. coli* FabH (PDB entry code: 5BNM) as a receptor model. The computational analysis revealed that compound **E4** with a binding energy of –37.4611 kcal/mol has an exceptional binding af-

Compound		E4		
Empirical formula	C ₂₃ H ₁₈ N ₂ O ₃	Z	2	
Temperature/K	223.00	D_{calcd} (Mg m ⁻³)	1.353	
Crystal system	monoclinic	μ (mm ⁻¹)	0.734	
Space group	P2 ₁	F(000)	388.0	
a (Å)	9.7698(10)	θ limits (°)	4.99 to 133.142	
b (Å)	5.2535(5)	Reflections collected	5820	
c (Å)	18.2571(18)	Independent reflections	2869 [$R_{\text{int}} = 0.0472$]	
a (°)	90	Data/restraints/parameters	2869/1/254	
β (°)	104.055(7)	GOF	0.959	
γ (°)	90	R_1/wR_2 [$I > 2\sigma Gs(I)$]	0.0998/ 0.2098	
Volume (Å ³)	909.00(16)	R_1/wR_2 (all data)	0.1144/ 0.2187	

Table 4. Crystal data and structure refinement for compound E4.

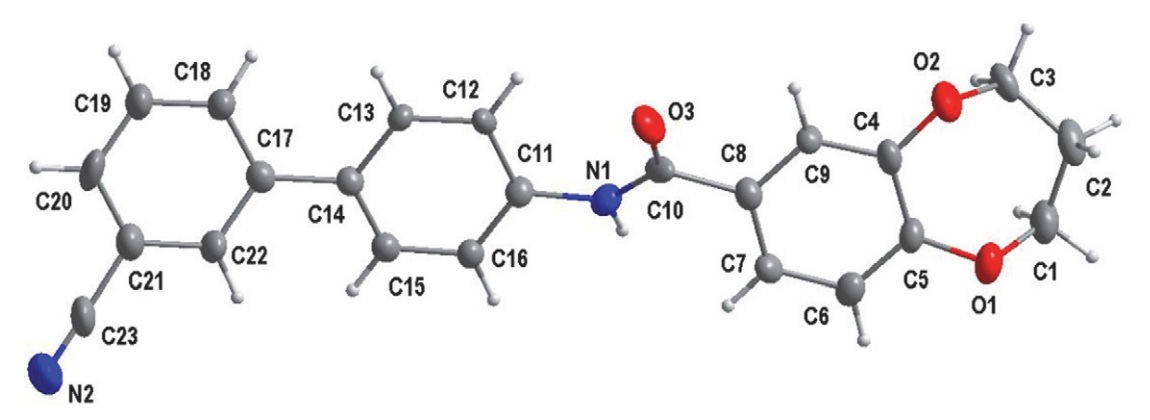


Figure 2. Crystal structure diagram of compound E4.

finity to the target protein FabH. Figure 3 shows the molecular docking visualization model of the target compound E4 with FabH, where panel A shows the hydrogen bonding interactions between the compound and the amino acid residues, and panels B and C show the 3D and 2D interaction diagrams of compound E4 with the amino acid residues. As shown in Figure 2, the amino acid residue ASN247 in the FabH protein forms a hydrogen bond with the carbonyl oxygen atom of the amide group of E4 (O... H-N; 3.23 Å). In addition, the nitrile group on the biphenyl group forms a hydrogen bond with the amino acid residue CYS112 (N...H-O; 2.76 Å). In addition, the amino acid residue ASN can also form a π -donor hydrogen bond with the first benzene ring of the biphenyl. At the same time, the first benzene ring of the biphenyl is able to form π - σ forces with the MET207 residue of FabH, while the second benzene ring forms π - σ forces with residues ALA246 and VAL212 and π-sulfur interactions with CYS1112. These interactions emphasize the crucial role of the amide backbone and the nitrile-substituted biphenyl in target binding. In addition, other interactions between various residues of 5BNM, including AGR36, ILE156 and ALA212, such as alkyl and π -alkyl interactions, further facilitated the binding interaction between compound E4 and FabH.

studies with the FabH receptor model of *E. coli*. The computational analysis revealed a significant binding affinity of compound **E4** to the FabH target, interacting with several residues. These results not only highlight the potential antimicrobial mechanism of **E4**, but also provide the basis for future research to develop similar benzodioxepine-carboxamide biphenyl derivatives to explore efficient antimicrobial lead compounds.

4. Experimental Section

4. 1. Materials and Measurements

All chemicals used were purchased and used without further purification unless otherwise stated. Silica gel (Qingdao Haiyang Chemical) with a mesh size of 200–300 was used for column chromatography. Analytical thin-layer chromatography (TLC) was performed on Huanghai silica gel plates with HSGF 254. UV light (254 nm or 365 nm) was used to detect all compounds. Separation of compounds by column chromatography was performed using silica gel 60 (200–300 mesh ASTM, E. Merck). The amount of silica gel used was 50 to 100 times the weight applied to the column. ¹H and ¹³C NMR data were recorded using a Bruker 400 MHz nuclear magnetic resonance spectrometer unless oth-

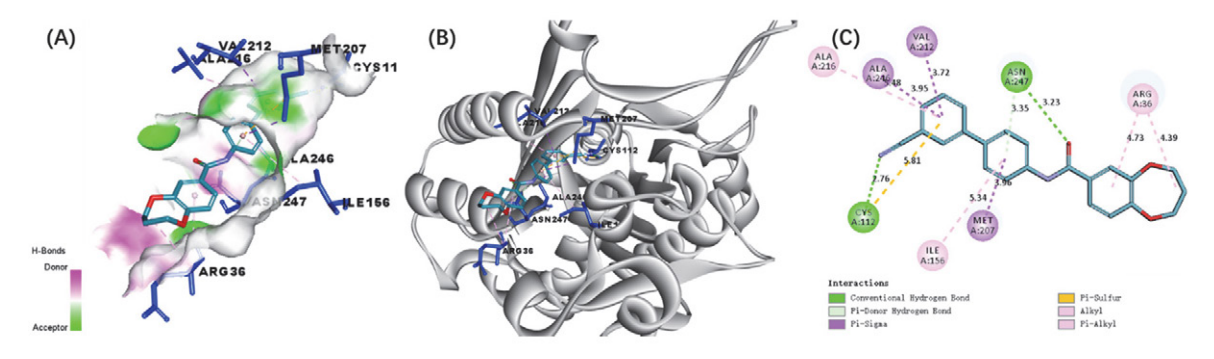


Figure 3. Molecular docking visualization model of the target compound E4 with FabH: (A) the hydrogen bonds between compound E4 and the amino acid residues, (B) and (C) the 3D and 2D interaction diagrams of compound E4 with the amino acid residues of FabH.

3. Conclusion

In this study, we carefully optimized the experimental conditions to determine the optimal parameters for the Suzuki coupling of compound **D** with phenylboronic acid. After establishing these conditions, we expanded the substrate range, resulting in the synthesis of eight new benzodioxepine-carboxamide biphenyl derivatives. The antimicrobial activity of these derivatives was evaluated and showed different inhibitory effects against *Escherichia coli*, *Pseudomonas fluorescens*, *Bacillus subtilis* and *Staphylococcus aureus*. In particular, compound **E4** showed the strongest antibacterial activity. To further investigate the potential of **E4** as an inhibitor of the FabH enzyme, we obtained its crystal structure and performed molecular docking

erwise stated. Chemical shifts are expressed in ppm (δ) using the residual solvent line as an internal standard. The splitting patterns are labeled s for singlet, d for doublet, t for triplet and m for multiplet. The ESI-MS spectra were recorded using a Mariner System 5304 mass spectrometer.

4. 2. Method for Preparing Compound D

The comprehensive synthesis of compounds **B** and **C**, including the respective yields, nuclear magnetic resonance (NMR) and mass spectrometry (MS) data, has already been documented in our research work. We therefore avoid redundant repetition of this information in this context. For the synthesis of the diazirinamide compounds, a dry 25 mL round bottom flask was equipped

with a magnetic stirrer. Compound **C** (97 mg, 0.5 mmol) was added to the flask along with the corresponding diazirinamine (0.5 mmol) and DMAP (1.1 equiv.) and then stirred in 2 mL dichloromethane at room temperature for 15 minutes. EDC·HCl (1.1 equiv.) was then added and stirred overnight. The resulting reaction mixture was diluted with 5 mL CH₂Cl₂ and filtered through a celite pad. The filtrate was further diluted with water (8 mL). After separation of the layers, the organic layer was washed with an aqueous saturated salt solution and then dried with Na₂SO₄. The organic layer was concentrated under reduced pressure, yielding the crude material, which was purified by column chromatography on silica gel. The structure elucidation of compound **D** was confirmed by ¹H NMR and ESI-HRMS.

N-(4-bromophenyl)-3,4-dihydro-2H-benzo[b][1,4]diox-epine-7-carboxamide (D)

White solid, yield 81%. m.p. 138.8-139.0 °C. IR (cm⁻¹) v 3324 (NH), 2973 (CH_{Ar}), 1655 (C=O), 1503 (C=C_{Ar}), 1323 (C-N), 1271, 1063 (=C-O-C). ¹H NMR (400 MHz, DMSO- d_6) δ : 7.73 (s, 1H), 7.56–7.49 (m, 2H), 7.49–7.42 (m, 3H), 7.43 (dd, J = 8.3, 2.3 Hz, 1H), 7.02 (d, J = 8.3 Hz, 1H), 4.29 (dt, J = 12.9, 5.8 Hz, 4H), 2.30–2.19 (m, 2H). ¹³C NMR (101 MHz, DMSO- d_6) δ 163.66, 153.07, 149.59, 135.89, 130.76, 128.22, 121.11, 120.54, 120.49, 119.59, 115.78, 69.26, 69.15, 29.91. ESI-HRMS m/z: 348.0222 [M+H]⁺, calcd for [C₁₆H₁₅BrNO₃]⁺: 348.0230.

4. 3. General method for preparing compound E

Under an inert nitrogen atmosphere, the synthesis procedure was initiated by adding the reactants one after the other to a three-necked flask: the intermediate **D** (50 mg, 0.14 mmol, 1.0 equiv.), a phenylboronic acid derivative (20.5 mg, 1.2 equiv.), Pd(dppf)Cl₂·DCM (12 mg, 5 mol%) and Cs₂CO₃ (94 mg, 2.0 equiv.), supplemented with a 2 ml aqueous solution of 1,4-dioxane (ratio 1:20 v/v). The mixture was then heated to 80 °C and kept under reflux conditions for 5 hours. After completion of the reaction and subsequent cooling to room temperature, the process was terminated by adding 10 ml of water. The reaction medium was then extracted three times in succession with dichloromethane and the organic layer was purified by washing with saturated sodium chloride solution. Concentration of the CH2Cl2 extract under reduced pressure by rotary evaporation yielded a crude product, which was subsequently purified by column chromatography to isolate the desired target compounds E1-E8.

N-([1,1'-biphenyl]-4-yl)-3,4-dihydro-2H-benzo[b][1,4] dioxepine-7-carboxamide (E1)

White solid, yield 90%. m.p. 163.1–163.9 °C. IR (cm⁻¹) ν 3362 (NH), 2927 (CH_{Ar}), 1661 (C=O), 1500 (C=C_{Ar}),

1321 (C-N), 1278, 1048 (=C-O-C). ¹H NMR (400 MHz, CDCl₃) δ 8.96 (s, 1H), 8.44 (td, J = 8.1, 1.7 Hz, 1H), 7.60 (d, J = 8.4 Hz, 2H), 7.43 (d, J = 8.4 Hz,2H), 7.16–7.02 (m, 2H), 7.01 (s, 2H), 6.89–6.81 (m, 2H), 6.67 (dd, J = 8.3, 2.2 Hz, 1H), 4.18 (dt, J = 17.1, 5.7 Hz, 4H), 2.15 (p, J = 5.7 Hz, 2H). ¹³C NMR (101 MHz, CDCl₃) δ 163.54, 152.95, 149.59, 139.25, 136.06, 136.03, 128.58, 127.54, 126.43, 125.87, 125.61, 121.08, 120.48, 119.53, 119.16, 69.25, 69.13, 29.93. ESI-HRMS m/z: 346.1433 [M+H]⁺, calcd for $[C_{22}H_{20}NO_3]^+$: 346.1438.

N-(3'-chloro-[1,1'-biphenyl]-4-yl)-3,4-dihydro-2H-ben-zo[b][1,4]dioxepine-7-carboxamide (E2)

White solid, yield 93%. m.p. 181.3-182.5 °C. IR (cm⁻¹) v 3394 (NH), 2956 (CH_{Ar}), 1665 (C=O), 1532, 1497 (C=C_{Ar}), 1310 (C-N), 1271, 1046 (=C-O-C), 786 (C-Cl). ¹H NMR (400 MHz, CDCl₃) δ 7.77 (s, 1H), 7.74–7.68 (m, 2H), 7.61–7.54 (m, 3H), 7.51 (d, J = 2.3 Hz, 1H), 7.52–7.43 (m, 2H), 7.34 (s, 1H), 7.40–7.27 (m, 1H), 7.05 (d, J = 8.3 Hz, 1H), 4.36–4.26 (m, 4H), 2.26 (p, J = 5.8 Hz, 2H). ¹³C NMR (101 MHz, CDCl₃) δ 164.76, 154.27, 150.87, 142.34, 137.86, 135.78, 134.70, 130.03, 127.71, 127.12, 126.96, 124.99, 122.32, 121.78, 120.77, 120.40, 70.53, 70.40, 31.17. ESI-HRMS m/z: 402.0863 [M+Na]⁺, calcd for [C₂₂H₁₈ClNO₃Na]⁺: 402.0867.

N-(3'-nitro-[1,1'-biphenyl]-4-yl)-3,4-dihydro-2H-ben-zo[b][1,4]dioxepine-7-carboxamide (E3)

Gray-yellow solid, yield 87%. m.p. 174.2-175.1 °C. IR (cm⁻¹) v 3335 (NH), 2952 (CH_{Ar}), 1647 (C=O), 1518, 1497 (C=C_{Ar}), 1349 (Ar-NO₂), 1309 (C-N), 1268, 1047 (=C-O-C). ¹H NMR (400 MHz, CDCl₃) δ 8.45 (t, J = 2.1 Hz, 1H), 8.19 (dd, J = 7.7, 2.2 Hz, 1H), 7.92 (d, J = 7.7 Hz, 1H), 7.83–7.74 (m, 3H), 7.68–7.57 (m, 3H), 7.57–7.44 (m, 2H), 7.06 (d, J = 8.3 Hz, 1H), 4.31 (dt, J = 11.2, 5.7 Hz, 4H), 2.25 (p, J = 5.7 Hz, 2H). ¹³C NMR (101 MHz, CDCl₃) δ 164.78, 154.36, 150.89, 148.80, 138.50, 134.52, 132.70, 129.76, 129.56, 127.83, 122.33, 121.86, 121.82, 121.59, 120.78, 120.53, 70.54, 70.40, 31.14. ESI-HRMS m/z: 413.1103 [M+Na]⁺, calcd for [C₂₂H₁₈N₂O₅Na]⁺: 413.1113.

N-(3'-cyano-[1,1'-biphenyl]-4-yl)-3,4-dihydro-2H-ben-zo[b][1,4]dioxepine-7-carboxamide (E4)

White solid, yield 79%. m.p. 169.5-170.1 °C. IR (cm⁻¹) v 3331 (NH), 2965 (CH_{Ar}), 2227 (C \equiv N), 1646 (C=O), 1527, 1497 (C=C_{Ar}), 1306 (C-N), 1267, 1049 (=C-O-C).

¹H NMR (400 MHz, CDCl₃) δ 7.86 (d, J = 1.8 Hz, 1H), 7.84–7.78 (m, 2H), 7.75 (d, J = 8.5 Hz, 2H), 7.65–7.44 (m, 6H), 7.06 (d, J = 8.3 Hz, 1H), 4.31 (dt, J = 11.2, 5.7 Hz, 4H), 2.26 (p, J = 5.8 Hz, 2H). ¹³C NMR (101 MHz, CDCl₃) δ 164.83, 154.34, 150.87, 141.73, 138.39, 134.72, 131.17, 130.51, 130.36, 129.65, 129.58, 127.71, 122.35, 121.79, 120.80, 120.57, 118.87, 113.00, 70.53, 70.40, 31.15. ESI-HRMS m/z: 371.1392 [M+H]⁺, calcd for [C₂₃H₁₉N₂O₃]⁺: 371.1390.

N-(3'-(trifluoromethoxy)-[1,1'-biphenyl]-4-yl)-3,4-dihy-dro-2H-benzo[b][1,4]dioxepine-7-carboxamide (E5)

Light yellow solid, yield 91%. m.p. 176.0–176.9 °C. IR (cm⁻¹) v 3388 (NH), 2964 (CH_{Ar}), 1663 (C=O), 1533, 1498 (C=C_{Ar}), 1313 (C-N), 1181, 1177 (C-F), 1265, 1045 (=C-O-C). ¹H NMR (400 MHz, CDCl₃) δ 7.79 (s, 1H), 7.76–7.68 (m, 2H), 7.62–7.52 (m, 2H), 7.55–7.40 (m, 5H), 7.19 (ddt, J = 8.1, 2.3, 1.1 Hz, 1H), 7.05 (d, J = 8.3 Hz, 1H), 4.30 (dt, J = 11.3, 5.7 Hz, 4H), 2.25 (p, J = 5.8 Hz, 2H). ¹³C NMR (101 MHz, CDCl₃) δ 164.77, 154.29, 150.87, 149.75, 142.61, 137.98, 135.61, 130.11, 129.68, 127.75, 125.18, 122.32, 121.78, 120.77, 120.44, 119.39, 70.52, 70.39, 31.16. ESI-HRMS m/z: 452.1082 [M+Na]⁺, calcd for [C₂₃H₁₈F₃NO₄Na]⁺: 452.1086.

N-(3'-(trifluoromethyl)-[1,1'-biphenyl]-4-yl)-3,4-dihydro-2H-benzo[b][1,4]dioxepine-7-carboxamide (E6)

White solid, yield 83%. m.p. 173.4–174.2 °C. IR (cm⁻¹) v 3327 (NH), 2961 (CH_{Ar}), 1645 (C=O), 1526, 1498 (C=C_{Ar}), 1313 (C-N), 1158 (C-F), 1267, 1060 (=C-O-C).

¹H NMR (400 MHz, CDCl₃) δ 7.83 (s, 1H), 7.80–7.70 (m, 4H), 7.65–7.56 (m, 2H), 7.55 (t, J = 7.6 Hz, 2H), 7.52 (d, J = 2.3 Hz, 1H), 7.47 (dd, J = 8.3, 2.3 Hz, 1H), 7.05 (d, J = 8.3 Hz, 1H), 4.31 (dt, J = 10.5, 5.8 Hz, 4H), 2.26 (p, J = 5.7 Hz, 2H).

¹³C NMR (101 MHz, CDCl₃) δ 164.75, 154.30, 150.88, 141.28, 138.02, 135.70, 131.38, 130.12, 129.67, 129.28, 127.81, 123.80, 123.57, 122.32, 121.80, 120.76, 120.46, 70.53, 70.40, 31.16. ESI-HRMS m/z: 414.1318 [M+H]⁺, calcd for [C₂₃H₁₉F₃NO₃]⁺: 414.1312.

N-(3'-chloro-5'-(trifluoromethyl)-[1,1'-biphenyl]-4-yl)-3,4-dihydro-2H-benzo[b][1,4]dioxepine-7-carboxamide (E7)

White solid, yield 88%. m.p. 143.8-144.2 °C. IR (cm⁻¹) v 3330 (NH), 2964 (CH_{Ar}), 1652 (C=O), 1521, 1496 (C=C_{Ar}), 1336 (C-N), 1127 (C-F), 1260, 1060 (=C-O-C), 825 (C-Cl). ¹H NMR (400 MHz, CDCl₃) δ 7.83 (s, 1H), 7.79–7.72 (m, 3H), 7.70 (s, 1H), 7.58 (dd, J = 9.0, 2.1 Hz, 3H), 7.52 (d, J = 2.3 Hz, 1H), 7.47 (dd, J = 8.3, 2.3 Hz, 1H), 7.05 (d, J = 8.3 Hz, 1H), 4.31 (dt, J = 11.6, 5.7 Hz, 4H), 2.26 (p, J = 5.8 Hz, 2H). ¹³C NMR (101 MHz, CDCl₃) δ 163.96, 153.51, 150.03, 137.76, 134.51, 133.35, 131.64, 129.30, 128.68, 126.95, 123.10, 123.06, 121.50, 121.01, 120.98, 120.95, 119.94, 119.66, 69.68, 69.54, 30.29. ESI-HRMS m/z: 448.0933 [M+H]+, calcd for [C₂₃H₁₈ClF₃NO₃]+: 448.0922.

N-(3',5'-dichloro-[1,1'-biphenyl]-4-yl)-3,4-dihydro-2H-benzo[b][1,4]dioxepine-7-carboxamide (E8)

White solid, yield 95%. m.p. 155.7–156.4 °C. IR (cm⁻¹) v 3376 (NH), 2935 (CH_{Ar}), 1663 (C=O), 1536, 1502 (C=C_{Ar}), 1334 (C-N), 1127 (C-F), 1272, 1062 (=C-O-C), 795 (C-Cl). ¹H NMR (400 MHz, CDCl₃) δ 7.77 (s, 1H), 7.72 (d, J = 8.6 Hz, 2H), 7.58–7.51 (m, 2H), 7.54–7.44 (m, 3H), 7.45 (s, 1H), 7.32 (t, J = 1.9 Hz, 1H), 7.05 (d, J = 8.3 Hz, 1H), 4.31 (dt, J = 11.2, 5.7 Hz, 4H), 2.26 (p, J = 5.8 Hz,

2H). 13 C NMR (101 MHz, CDCl₃) δ 164.79, 154.33, 150.87, 143.46, 138.40, 135.31, 134.38, 129.58, 127.71, 126.96, 125.30, 122.33, 121.79, 120.79, 120.43, 70.53, 70.39, 31.15. ESI-HRMS m/z:414.0667 [M+H]⁺, calcd for [C₂₂H₁₈Cl₂NO₃]⁺: 414.0658.

4. 4. In vitro Bacterial Suppressive Assay

To evaluate the in vitro activity of the compounds, the tetrazolium reduction assay was performed with thiazolyl blue tetrazolium bromide (MTT) using the TTC double dilution method. Nutrient broth (NB) was used as the medium for bacterial growth. Seeding broth containing microbial spores was prepared in NB with 24-hour-old bacterial cultures on nutrient agar (Hi-media) and incubated at 37 °C. The bacterial suspension was then adjusted with sterile saline to a concentration of 1×10^4 to 1×10^5 colony forming units (CFU)/mL. The tested compounds and the reference drugs were serially diluted twice to obtain the desired concentrations of 100, 50, 12.5, 6.25, 3.13 and 1.56 µg/mL. The tubes were then incubated in BOD incubators at 37 °C for the bacterial strains. The minimum inhibitory concentrations (MIC) were determined based on visual observations after a 24-hour incubation period for the bacteria.

4. 5. Cytotoxicity Test

Cytotoxic in vitro activity was investigated using the MTT assay against NIH-3T3 mouse fibroblast cells. Cells were cultured in a 96-well plate at a density of 5×10^3 cells per well, and different concentrations of the compounds were added to each well. After a 24-hour incubation at 37 °C under a 5% CO₂ atmosphere, cytotoxicity was assessed. In addition, 20 μL of MTT reagent (4 mg/mL) was added to each well 4 hours before the end of the incubation period. After four hours, the plate was centrifuged at 1200 rpm for 5 minutes, the supernatant was removed and 200 μL of DMSO was added to each well. The absorbance was then measured at a wavelength of 570 nm (OD₅₇₀ nm) using an ELISA microplate reader. Three replicate wells were used for each concentration and each test was performed three times so that the average IC₅₀ value could be calculated. The cytotoxicity of each compound was expressed as the concentration at which cell viability was reduced by 50% $(IC_{50}).$

4. 6. Experimental Protocol for Docking Study

In the molecular docking analysis, compound **E4** was inserted into the three-dimensional X-ray structure of *E. coli* FabH (PDB: 5BNM) using the Discovery Studio Client (v19.1.0). The DS-CDOCKER protocol was used via the graphical user interface to facilitate this process. To generate accurate representations of the compounds in

three dimensions, Chem. 3D ultra 12.0 from Cambridge Soft Corporation, USA, which follows the Chemical Structure Drawing Standard, was used. To optimize the energy of the constructed structures, the MMFF94 force field was used, and the iterations were set to 5000 with a minimum RMS gradient of 0.10. For the comparative analysis, the crystal structures of the *E. coli* FabH (PDB: 5BNM) complex were taken from the RCSB Protein Data Bank (http://www.rcsb.org/pdb/). Prior to analysis, all water molecules and ligands bound to the protein were removed in order to focus exclusively on the interaction of interest. In addition, polar hydrogen atoms were added to the protein structures to ensure accurate representation of hydrogen bonding interactions.

Acknowledgments

This work was supported by the S&T Innovation 2025 Major Special Program of Ningbo (2020Z091), the Natural Science Foundation of China (22007090) and Shenzhen High-tech Zone Development Special Plan Pingshan District Innovation Platform Construction Project (29853MKCJ202300208), Natural Science Foundation of Ningbo (2019A610190), the Basic Public Welfare Research Program of Zhejiang Province (LGF21H180012).

Conflict of Interests

The authors do not report any conflicts of interest in this work.

Supplementary Data

CCDC 2348536 contains the additional crystallographic data for compound E4. These data are available free of charge at http://www.ccdc.cam.ac.uk/conts/retrieving. html, or from the Cambridge Crystallographic Data Center, 12 Union Road, Cambridge CB2 1EZ, UK; fax: (+44) 1223-336-033; or e-mail: deposit@ccdc.cam.ac. uk. The spectral data of the compounds can be found in the supporting information file.

5. References

- D. C. C. Carla, C. M. Jose, *Molecules*. 2018, 23, 2583.
 DOI:10.3390/molecules23102583
- A. N. Günenc, B. Graf, H. Stark, A. Chari. Subcell Biochem.
 2022, 99, 1–33. DOI:10.1007/978-3-031-00793-4_1
- C. Wu, B. Hong, S. S. Jiang, X. Luo, H. Lin, Y. Zhou, J. R. Wu, X. Q. Yue, H. S. Shi, R. N. Wu, *Biochem. Eng. J*, 2022, 178, 108306. DOI:10.1016/j.bej.2021.108306
- J. W. Yao, C. O. Rock, Biochim. Biophys. Acta BBA Mol. Cell Biol. Lipids. 2017, 1862, 1300–1309.
 DOI:10.1016/j.bbalip.2016.09.014
- 5. M. F. Currie, D. M. Persaud, N. K. Rana, A. J. Platt, J. Beld, K.

- L. Jaremko, *Sci. Rep.* **2020**, *10*, 17776. **DOI:**10.1038/s41598-020-74731-4
- F. Asturias, J. Chadick, I. Cheung, H. Stark. A. Witkowski. A. Joshi. S. Smith. *Nat. Struct. Mol. Biol.* 2005, *12*, 225–232.
 DOI:10.1038/nsmb899
- O. S. Ostroumova, S. S. Efimova, *Antibiotics*. 2023, *12*, 1716.
 DOI:10.3390/antibiotics12121716
- 8. N. Risa, P. Benjamin, N. Yosi, M. Taifo, *MedChemComm*. **2019**, *10*, 1517–1530. **DOI:**10.1039/C9MD00162J
- 9. X. Y. Lu, J. Tang, Z. Zhang, K. Ding, Curr. Med. Chem. 2015, 22, 651–667.
 - **DOI:**10.2174/0929867322666141212115236
- C. Davies, R. J. Heath, S. W. White, C. O. Rock, Struct. 2000, 8, 185–195. DOI:10.1016/S0969-2126(00)00094-0
- X. Y. Qiu, A. E. Choudhry, C. A. Janson, M. Grooms, R. A. Daines, J. T. Lonsdale, S. S. Khandekar, *Protein Sci. Publ. Protein Soc.* 2005, 14, 2087–2094. DOI:10.1110/ps.051501605
- W. C. Lee, M. C. Jeong, Y. Lee, C. Kwak, J. Y. Lee, Y. Kim, Mol. Microbiol. 2018, 108, 567–577. DOI:10.1111/mmi.13950
- Y. Zhou, Q. R. Du, J. Sun, J. R. Li, F. Fang, D. D. Li, Y. Qian, H. B. Gong, J. Zhao, H. L. Zhu, *ChemMedChem.* 2013, 8, 433–441. DOI:10.1002/cmdc.201200587
- Y. Zhou, Y. Luo, Y. S. Yang, L, Lu, H. L. Zhu, MedChemComm.
 2016, 7, 1980–1987. DOI:10.1039/C6MD00263C
- Y. Zhou, Y. S. Yang, X. D. Song, L. Lu, H. L. Zhu, Chem. Pharm. Bull. 2017, 65, 178–185. DOI:10.1248/cpb.c16-00772
- H. Y. Chang, R. Y. Ji, Z. Y. Zhu, Y. P. Wang, S. P. Yan, D. He, Q. K. Jia, P. Huang, T. Cheng, R. Wang, Y. Zhou, *Eur. J. Med. Chem.* 2024, 265, 116064. DOI:10.1016/j.ejmech.2023.116064
- Y. Gao, J. Yang, X. L. Yang, L. Zhang, J. Wang, Q. Li, D. M. Lin, M. Zhang, S. N. Xia, L. L. Xu, Q. Zhang, P. Hai, Y. H. Liu, S. Wang, L. P. Guo, *Fitoterapia*. 2021, 152, 104914.
 DOI:10.1016/j.fitote.2021.104914
- C. G. Song, X. Wang, J. Yang, Y. Kuang, Y. X. Wang, S. X. Yang,
 J. C. Qin, L. P. Guo, *Chem. Biodivers.* **2021**, *18*, e2100079.
 DOI:10.1002/cbdv.202100079
- X. Wang, H. Y. Fu, W. He, Y. T. Xiang, Z. C. Yang, Y. Kuang, S. X. Yang, Curr. Issues Mol. Biol. 2022, 44, 4087–4099.
 DOI:10.3390/cimb44090280
- A. J. Tague, P. Putsathit, T. V. Riley, P. A. Keller, S. G. Pyne, *ACS Med. Chem. Lett.* 2021, 12, 413–419.
 DOI:10.1021/acsmedchemlett.0c00611
- S. Y. Ke, Z. L. Gao, Z. G. Zhang, F. Liu, S. H. Wen, Y. Y. Wang,
 D. Y. Huang, J. Agric. Food Chem. 2023, 71, 14505–14516.
 DOI:10.1021/acs.jafc.3c04307
- 22. A. Marta, R. Laura B, V. Albert, H. Sonia, A. Lidia, M. Mar, V. Henar, T. Carlos, R. Erney, H. Annabelle, N. Matthew, B. Isabel, C. Pablo, S. Steven A, A. Jose M, L. Maria L, ACS Chem. Biol. 2015, 10, 834–843. DOI:10.1021/cb500974d
- Y. Guo, E. H. Hou, T. Y. Wen, X. T. Yan, M. Y. Han, L. P. Bai,
 X. G. Fu, J. F. Liu, S. S. Qin, *J. Med. Chem.* 2021, 64, 12903–12916. DOI:10.1021/acs.jmedchem.1c01073
- 24. X. N. Chen. W. Q. Lan. J. Xie. Food Chem. 2024, 440, 138198.
 DOI:10.1016/j.foodchem.2023.138198
- Z. J. Jain. P. S. Gide. R. S. Kankate. *Arab. J. Chem.* 2017, 10, S2051–S2066. DOI:10.1016/j.arabjc.2013.07.035

26. H. Ibrar, C. Jawoeski, Y. Mirza A, *Adv. Synth. Catal.* **2016**, *358*, 3320–3349. **DOI**:10.1002/adsc.201600354

27. Z. F. Han, J. S. Pinkner, B. Ford, R. Obermann, W. Nolan, S. A. Wildman, D. Hobbs, T. Ellenberger, C. K. Cusumano, S. J. Hultgren, J. W. Janetka, *J Med. Chem.* 2010, 53, 4779–4792. DOI:10.1021/jm100438s

Povzetek

Biosinteza maščobnih kislin je pomembna presnovna pot v bakterijskih organizmih. Avtorji so v prejšnjih študijah že raziskovali protimikrobne spojine, zasidrane v ogrodju benzodioksepina, ki je znan po svojih izrazitih antibakterijskih lastnostih. Na podlagi teh znanj so avtorji zasnovali in sintetizirali serijo osmih inovativnih benzodioksepin-bifenil amidnih derivatov z optimizacijo sinteznih metod. Študija med drugim zajema tudi natančno oceno antibakterijskih lastnosti in biokompatibilnosti novih spojin. Predvsem spojina **E4** se je izkazala kot izjemno učinkovito protimikrobno sredstvo. Poleg podrobne analize kristalne strukture spojine **E4** je bila izvedena tudi temeljita študija sidranja, z namenom raziskati interakcije te spojine z encimom FabH.



Except when otherwise noted, articles in this journal are published under the terms and conditions of the Creative Commons Attribution 4.0 International License